

SoLID Detector Beam Test 2022-2023 Short Summary

X. Bai,¹ A. Camsonne,² J. Caylor,³ J.-P. Chen,² H. Gao,⁴ C. Hedinger,¹ N. Liyanage,¹
Z.-E. Meziani,⁵ M. Nycz,¹ S. Opatrny,¹ C. Peng,⁵ M. Paolone,⁶ P. A. Souder,³
Y. Tian,³ Z. Ye,⁷ D.W. Upton,¹ J. Zhang,¹ Z.-W. Zhao,⁴ and X. Zheng¹

¹*University of Virginia, Charlottesville, VA, USA*

²*Thomas Jefferson National Accelerator Facility, Newport News, VA, USA*

³*Syracuse University, Syracuse, NY, USA*

⁴*Duke University and Triangle Universities Nuclear Laboratory, Durham, NC, USA*

⁵*Argonne National Laboratory, Argonne, IL, USA*

⁶*New Mexico State University, Las Cruces, NM, USA*

⁷*Tsinghua University, Beijing, China*

(Dated: March 5, 2024)

This short report summarizes the SoLID Electromagnetic Calorimeter (ECal) beam test that was conducted from August 2022 through March 2023 in Hall C of Jefferson Lab. Data analysis is still ongoing. We present the setup of the beam test and a few preliminary findings, along with a list of results to be expected from the ongoing analysis. Our current results show that the ECal and SPD will be functioning at SoLID running conditions and their particle identification (PID) performance will satisfy SoLID physics program's requirement. This short report will be superseded by a full version once the analysis is completed. A separate analysis of AI/ML-based PID is being conducted in parallel and will be reported separately.

CONTENTS

I. Introduction	1
II. Experiment Setup	2
A. Detector Layout and Test Location	2
B. Details of the Detectors	3
C. GEM Readout	3
D. Cherenkov, Scintillator, and ECal Readout	4
E. Trigger Setup	5
F. FADC Data Processing	5
G. Test conditions (target, beam, radiation)	7
III. Simulation	7
IV. Preliminary Findings	7
A. Benchmarking simulations	7
B. Performance of shower passive base at high rate	8
C. Timing with FADC	9
V. Analysis to be Completed	9
VI. Summary and Outlook	9
References	10

I. INTRODUCTION

The Solenoidal Large Intensity Device (SoLID) [1] is a spectrometer designed to meet the need of frontier research in the area of nuclear strong force (QCD) and fundamental symmetries. In order to tackle topics such as imaging the substructure of the nucleon in multi-dimension and to study parity violation to high precision, high statistics are needed, which requires a spectrometer of large acceptance equipped with detectors that can resist high radiation and a data acquisition system (DAQ) that can handle high rate. SoLID was designed with all these requirements in mind, and will be installed in Jefferson Lab (JLab)'s Hall A, ideally after the MOLLER experiment is completed. Experiments that have been approved to run with SoLID includes measurement of the nucleon 3D structure through Semi-Inclusive Deep Inelastic Scattering (SIDIS), studies of the origin of the proton mass using near-threshold J/ψ production, and measurement of a set of electron-quark neutral-weak interaction couplings through parity violating DIS (PVDIS).

In the past few years, the SoLID collaboration has reached a baseline design of its detectors, and its Cherenkov detector components had been tested under a high background, high radiation environment. This writeup reports on a recent test of a nearly full set of SoLID's detectors – including large-angle scintillator-pad detector (LASPD), GEM, Cherenkov, and electromagnetic calorimeter (ECal) – in JLab's Hall C from mid-2022 through March 2023, with a focus on the ECal as well as general performance of all detectors under high back-

ground and high radiation.

High quality data were obtained with the detectors placed in an open area at 18° from the beamline, while supplemental data were also taken at 7° and 82° . The electron beam was 10.6 GeV and the beam current varied from 5 to $70 \mu\text{A}$, while the target varied from carbon foils to 10-cm long liquid deuterium or hydrogen. The luminosity of the 2022/23 beam test was below that of SoLID PVDIS experiment, but the low energy background incident on the detectors was comparable or above PVDIS. The beam test luminosity and background at the highest current were both higher than the SIDIS and J/ψ run conditions.

The data collected in this beam test will help to benchmark the simulation based on which the SoLID physics program was designed. The data rates agree with GEANT-based simulation to within 15% at both 7° and 18° . All of the scintillators and preshower detectors performed well and stable. The signal output of the shower modules exhibit unexpected behavior, though this is now understood and we believe can be mitigated by a specially-designed, radiation-hard active high-voltage divider base. Given that the ECal plays a critical role in the SoLID physics program, the particle identification performance of the ECal was extracted from the beam test data and our preliminary results were found to meet the requirements of the SoLID physics program. At present, data analysis is still ongoing, including simulation tuning and AI/ML-based PID analysis. In the following, we present the beam test setup in Section II, simulation in Section III, and preliminary findings in Section IV. We expect the full analysis of simulation and PID using classical method to be completed by the end of 2024, and AI/ML-based PID analysis in 2025 if sufficient resources are available.

II. EXPERIMENT SETUP

A. Detector Layout and Test Location

The hardware configuration for the SoLID detector beam test consisted of four scintillators, two pairs of GEMs, one Large-Angle Scintillator Pad Detector (LASPD), a CO_2 Cherenkov detector, and a Electromagnetic calorimeter (ECal) composed of three each of Preshower and Shower Modules. The LASPD, preshower, and shower modules were made to specification following the preliminary conceptual design report (pre-CDR) from 2019 [2]. All the detectors were attached to a test stand, see Fig. 1.

The detector test stand was placed in Hall C of JLab and was raised to the same height as the beam-

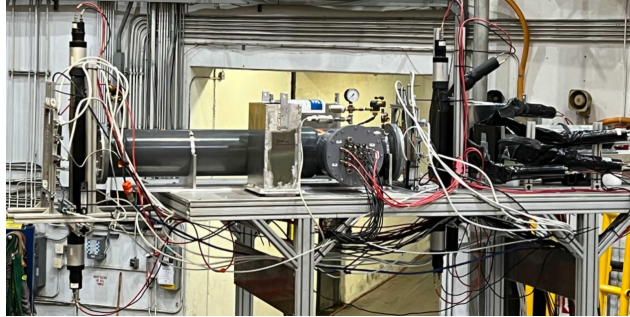


FIG. 1. Picture of the beam test detectors mounted on the test stand.

line. The test could be divided into three periods in time: From August to December 2022, the test stand were positioned on the left side (same side as the Super-High Momentum Spectrometer or SHMS) from the beamline at 82° . The setup had a reduced configuration (see below for details) and was for commissioning purposes. We call this the low-rate configuration hereafter. The stand was moved to a very small angle of 7° on the right side (same side as High Momentum Spectrometer or HMS) of the beamline during the winter break. However, the location had too high event rate and was not suitable for detector testing. In February 2023, the stand was moved further to 18° beam-right which is where the majority of high-quality test data were taken, see Fig. 2.

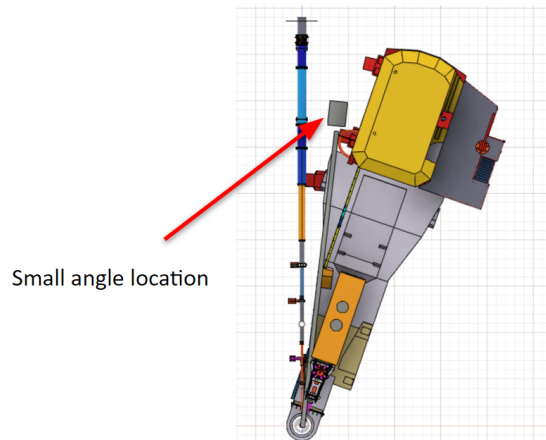


FIG. 2. Location of the test stand for the high-rate test of 2023. The stand (grey box) was position between the beamline and the High Momentum Spectrometer (HMS).

Detector	Size (cm)	thickness (cm)	Readout
GEM0	10 × 10	1.5	APV/mpd
GEM1	10 × 10	1.5	APV/mpd
SC-A	5.0(W) × 7.5(H)	1.0	PMT
Cherenkov	circular $\Phi 20$		4 MAPMTs
GEM2	10 × 10	1.5	APV/mpd
GEM3	10 × 10	1.5	APV/mpd
SC-C	18.0(W) × [3.5(L), 4.5(R)](H) trapezoid	2.0	LG+PMT (R)
LASPD	[8.3 (B), 14 (T)](W) × 57(H) trapezoid	2.0	LG+PMT (T,B)
SC-D	6.25-side hexagon	2.0	LG+PMT
pre-lead			--
Preshower	6.25-side hexagon	2.0	WLS fiber, PMT
Shower	6.25-side hexagon	45	WLS fiber, PMT
SC-B	5.0(H) × 10.0(W)	1.0	PMT

TABLE I. The size (both transverse and thickness) of each detector and their readout information.

B. Details of the Detectors

A schematic diagram of the detailed detector layout for the 18° test period is shown in Fig. 3. From front to back, the detectors are arranged in the order of: (poly shielding), GEM0, GEM1, Scintillator(SC)-A, Cherenkov, GEM2, GEM3, SC-C, LASPD, SC-D, Pre-lead, Preshower, Shower, and SC-B.

The exact size of each detector and details of the material is listed in Table I and illustrated in Fig. 4. Two of the scintillators have a trapezoid shape: SC-C is 18-cm wide and is 3.5 and 4.5 cm in height on the left- and right-side, respectively. The LASPD is 57 cm tall and is 8.3 cm and 14 cm wide at the bottom and top end, respectively. The three Preshower and Shower modules each have a hexagon-shape cross section and are arranged in a triangular formation, and are labeled as PSH-Left, Top, Right and SH-Left, Top, Right, respectively, viewing along the direction of particles incident on the front.

C. GEM Readout

The GEMs were read out using the MPD-APV system. The system was developed for Hall A SBS program, and a similar architecture was adopted for this beam test setup. The system contains three major parts: APV25-s1 chips for reading analog signals from GEM detectors, MPD (Multi Purpose Digitizer) modules for APV configuration and digitization, and an SSP (Subsystem Processor) module for trigger data process. Among these, the APV25-s1

is an analogue pipeline ASIC designed for reading silicon strip detectors, initially developed for CMS trackers; the chip contains 128 channels; each channel has its own independent pre-amplifier and shaper circuits; each channel is also equipped with a 192-depth buffer which will be continuously written by APV samples, no matter whether a trigger exists or not. While properly configured, the chip keeps sampling its input under the driving clock. The clock signal is provided by the MPD modules.

The MPD module is a 6U VME module designed by INFN for digitization and configuration. The core part on board is a powerful Altera ARRIA GX FPGA, which gives the module ability to handle up to 16 APVs for digitization and configuration. The MPD module provides a 41.6 MHz clock to all the APVs connected to it; thus, there are no APV synchronization issues on the same MPD module since they share the same clock. There are 2 different clock options for the MPD module, either generated locally by the MPD module or from the front panel input. In this beam test setup, we used the MPD local clock. Therefore, an external synchronization clock is needed between MPD modules for better synchronization. However, since GEM detector timing resolution is not a goal for this beam test, the synchronization clock is skipped in this setup. Owing to the powerful on-board FPGA, the MPD is also capable of doing online zero suppression, which can reduce the data volume significantly depending on occupancy. Due to the extra resources required by the online zero suppression, the FPGA resources for the 16th APV were reassigned to online zero suppression, leading to a maximum of 15 APVs for each MPD module. The online zero suppression is turned off in our setup since the total number of channels is small, and also we want full signals for better data quality.

The digitized data from MPD modules will be sent to an SSP module through a fiber link. The SSP module is a 6U VME module designed by JLab for its 12GeV experiments. One SSP module can handle up to 8 crates with the same type of detectors. Different types of detectors will require different SSP modules. For this beam test DAQ setup, the SSP module is dedicated to the GEM data; it combines the data streams from 4 MPD modules and sends the processed data to ROC through the VXS back-plane data path. The SSP module sits in the same VXS crate as the FADC modules for calorimeters, scintillators, etc. A specific ROC library was developed by Bryan Moffit (JLab) for reading SSP and FADC data simultaneously through the VXS back-plane data path.

In this beam test setup, a total of four 10 cm by 10 cm GEM chambers were used; each cham-

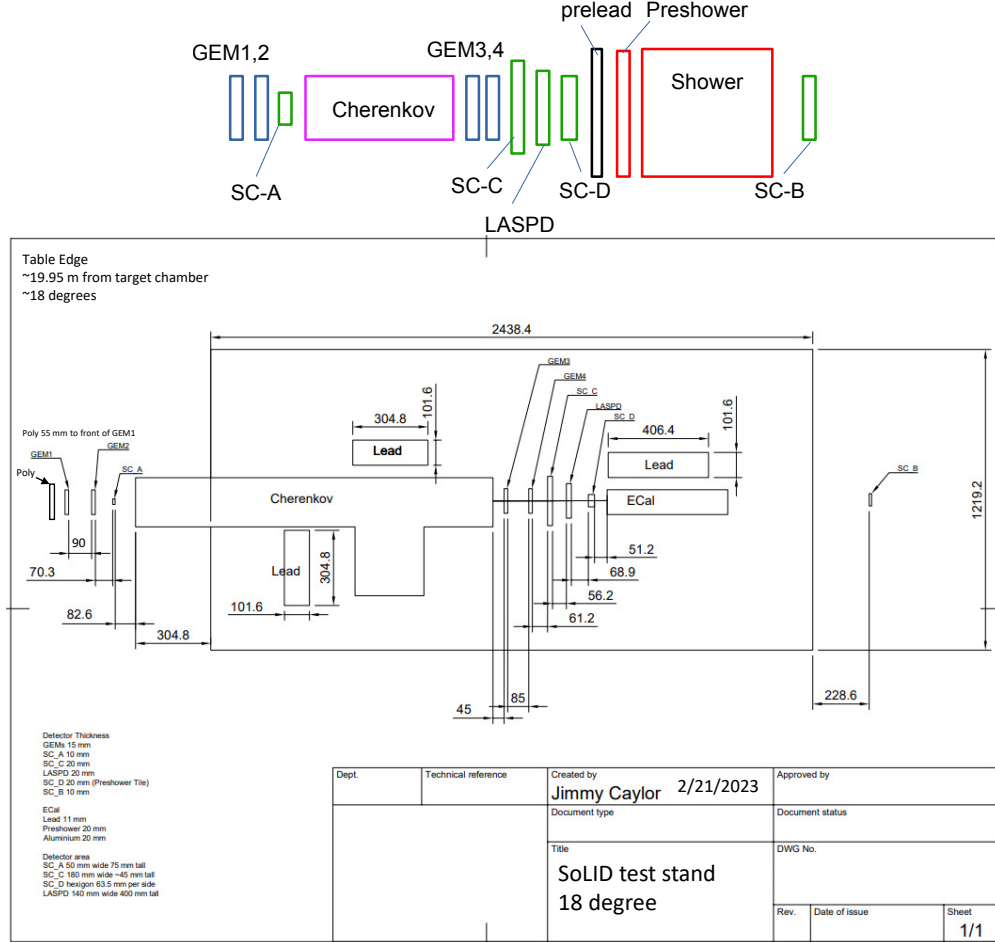


FIG. 3. Illustration of the detector layout, (top) and measurements of the relative positions of the components (bottom), for the high rate test period of 18° . Both are as viewed from above the detector stand. The particles enter from the left. The 7° test period had nearly identical layout with the exception of no poly shielding in front of the GEM at the front.

ber requires 4 APVs for readout, 2 per each GEM detector axis. The APVs are plugged into the 5-slot backplanes; the backplane is a PCB board designed by INFN, which serves as the bridge between the MPD modules and APV hybrid cards. The backplanes directly connect to MPD modules through HDMI cables. In this setup, each backplane only houses 2 APVs due to the small size of GEM chambers; one GEM detector axis requires one backplane. The I2C address and ADC channel address for each APV can be configured by a flip switch on the backplane. APVs on the same MPD module cannot have the same address; otherwise, data will be written to the same buffer, leading to a data race. Each 5-slot backplane contains 1 digital HDMI connector for the APV configuration and clock signal, and 1 analog HDMI connector for APV sending detector signals. On the other hand, each MPD module has 2 digital HDMI ports and 4 Analog HDMI ports;

this means that each 10 cm by 10 cm GEM chamber will use up all digital HDMI ports on one MPD module. Therefore, a total of 4 MPD modules were used in the DAQ setup, one MPD per chamber. A schematic diagram is provided in Fig 5 showing the gist of connections between different modules.

D. Cherenkov, Scintillator, and ECal Readout

Except for GEMs where were read out using the MPD-APV system as described in the previous section, each of the other detectors was connected to the required high-voltage (HV) and signals were collected with photo multiplier tubes (PMTs). All of SC-A,B,C,D were read out from the right side (opposite of the beamline during 18° run), some with and some without a light guide (LG), but all with an $\times 10$ amplifier. For the LASPD, each of the bot-

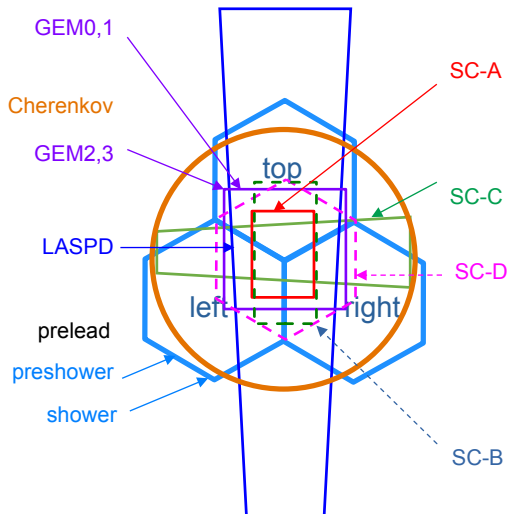


FIG. 4. Illustration of the detector transverse sizes as viewed from the front of the test stand. The poly shielding is not shown.

tom and the top sides was coupled to a Hamamatsu R9779 (assembly H10570) via a lightguide, with the top light guide bending the light by 55° .

The Cherenkov detector is a small prototype [3] used previously for testing Cherenkov readout. It was equipped with 4 reflecting mirrors (quadrants), each reflecting the light towards a 64-channel MAPMT. The quadrants A and D were equipped with two Hamamatsu H8500-03, and the quadrants B and C with two Hamamatsu H12700-03. Each 64-ch MAPMT was further divided into a 2×2 grid and each grid (16 pixel-channels) was sent to a FADC channel input. This results in a total of 16 FADC readouts for the Cherenkov.

The Preshower modules are 2-cm thick hexagon-shaped scintillator tiles with 1-mm diameter round WLS [Kuraray Y11(200)] fibers embedded on the tile surface for guiding the light out. The WLS fiber ends of each preshower tile were read out together using a PMT. The preshower modules are also labeled as prototype SDU2 (PreSh-Top), SDU1 (PreSh-L), and THU1 (PreSh-R).

The Shower modules, of shashlyk design, each has 97 WLS fiber ends coupled to a PMT (Beijing-Hamamatsu) and the PMT gain was characterized prior to the test, see Table II. The nominal HV setting for the three modules were 960 V (T), 860 V (L), and 1030 V (R), corresponding to a gain of about 2×10^5 for the main data taking period at 18° . The shower modules are also labeled as prototype SDU5 (Sh-Top), SDU4 (Sh-L), and THU2 (Sh-R).

Shower	PMT#	β	gain	HV (V)
SDU5 (Top)	CR284 52766	7.175	2×10^5	921
			2.5×10^6	1200
			3.4×10^6	1250
			4.61×10^6	1300
SDU4 (Left)	CR284 52654	7.497	2×10^5	875
			3.64×10^6	1180
			4.235×10^6	1200
			6.145×10^6	1260
THU2 (Right)	CR284 52610	6.928	2×10^5	1034
			5.11×10^6	1500
			1.246×10^7	1700

TABLE II. Shower module labeling and gain characterization of their readout PMTs. Two of the prototypes were made by Shandong University (SDU) and one by Tsinghua University (THU).

E. Trigger Setup

Once all detector signals are collected by PMTs, they were first split by summing modules (CAEN N625) to make two identical copies of each. One copy was sent to Flash ADCs of 4-ns sampling rate (JLab FADC250) for readout, and another copy was used to form trigger signals. Three hardware-based sums were formed: one (CerSum) was the sum of all 16 channels of Cherenkov signals, one (PshSum) for the sum of the three preshower modules, and one (ShSum) for the sum of the three shower modules. For the 18° run, a total of four trigger signals were formed, see Table III. Note that the Trigger signals TS1, 2, 3, 4 correspond to the lowest four bits of the trigger module (JLab TI1), which were decoded as Trigger Type 1, 2, 4, 8, respectively, in the data stream. To avoid confusion, we will use the Trigger signal naming scheme hereafter. TS1 is a potential electron trigger the requires CerSum above 2 photo-electrons. TS2 is a potential pion trigger due to the requirement of a signal in SC-B located behind the Shower modules, though high-energy electrons could also leak through the calorimeter and trigger it. TS3 is a charged particle trigger, requiring two scintillators firing. TS4 is aimed for both electrons and neutral particles (mostly photons both from the target and from π^0 decay) with limited energy selection by adjusting the threshold in the ShSum.

F. FADC Data Processing

All trigger and FADC data were sent to a PC equipped with the standard CODA [1]. The FADC range (4096 or 12-bit) was set to 2V for the Shower. For Cherenkov, the range was 2V for the earlier run period, which was changed to 1V on March 1,

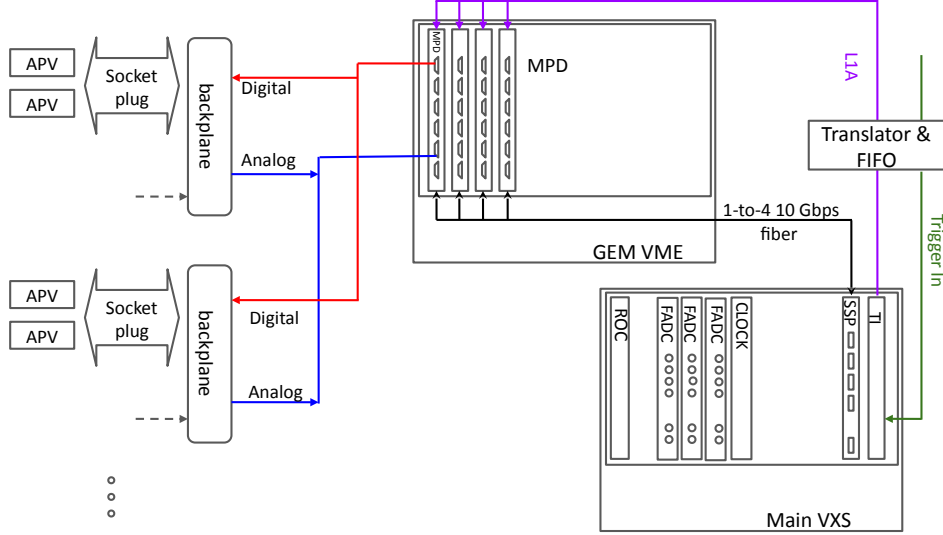


FIG. 5. GEM DAQ setup with the gist of connections between different modules

Trigger Signal	Bit	Trig -Type	Trigger Logic (threshold)	Goal
TS1	0001	1	C Sum (35mV) (≈ 2 PE)	e
TS2	0010	2	SC-B (35mV).and.SC-D(35mV) (≈ 0.5 MIP each)	π^\pm
TS3	0100	4	SC-C(31mV).and.SC-D(35mV) .and.ShSum (varies)	e, π^\pm
TS4	1000	8	ShSum (varies)	e or γ

TABLE III. Trigger setup for the majority of the 18° data taking. The threshold for each of SC-B, SC-C and SC-D corresponds approximately to half of MIP. SC-A was initially in TS2, but was found to saturate and later removed.

2023 (starting run 4376) for the majority of the 18° data taking. The range for Preshower was similarly settled at 0.5V for the 18° data taking. The processing of FADC data starts with the raw waveform (level0 data) analysis. A peak-finding algorithm was used: The FADC waveform was scanned and the time-derivative of the signal was used to determine whether a peak has started (positive derivative) or ended (negative derivative). Alternatively, the integration time can be set at a fixed value for individual detectors to avoid misidentifying the peak ending time due to signal pile-ups. The decoder stores the starting- and end-time, the height, and the time-integral of each peak. In addition, a special edge-finding algorithm can be used to determine the peak starting time without the need of time-walk corrections, see Section IV C for details.

By integrating the peaks of the level0 tree, we obtain information such as peak integral, height, and

start/ending time and the peak width. At high rate, a “baseline” is also extracted which would be higher than the pedestal due to background pileup.

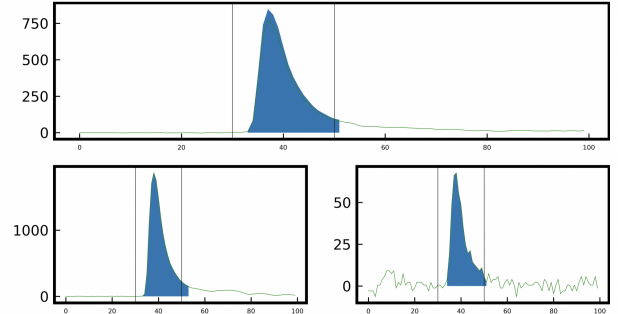


FIG. 6. Subplots show the waveform from level0 tree for each of the Shower modules (left, top, and right). From this, we see pedestal seems to fluctuate on the order of 20 FADC units, thus large values can easily be distinguished from noise while small signals become indistinguishable. This factors into the peak-finding algorithm, which uses different user-specified (software) thresholds to best determine peaks and integrate over the appropriate timing-windows.

Because the FADC signals contain waveform for a total of 400 ns window (100 samples), additional information was obtained by studying the waveform before the trigger signal arrives, i.e. “out of time window” waveform. This provided an independent check of the analysis, and was particularly useful for small signals which would be rejected by the peak-finding algorithm due to small amplitudes.

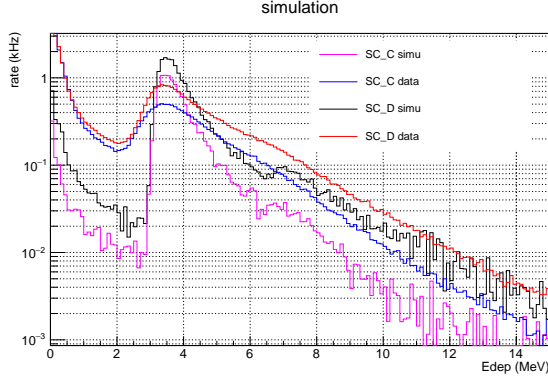


FIG. 9. The SC_C and SC_D distributions with TS4 trigger with a 15-mV threshold. The data were taken with a LD₂ target at 10 μ A and are compared with corresponding simulated spectra with a ShowerSum > 0.5 MIP cut.

extract low-energy particle signals that would not pass the trigger threshold. Overall, the agreement between data and simulation is excellent.

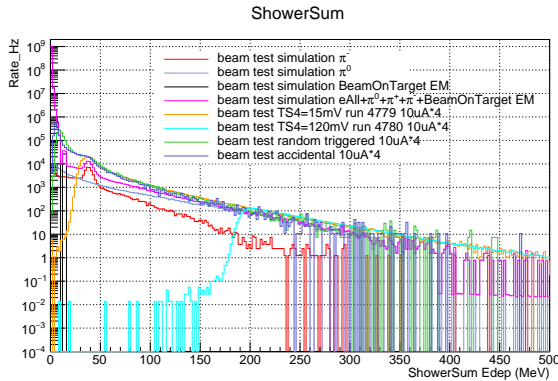


FIG. 10. The zoom version of simulated ShowerSum distributions for the beam test with 10cm LD₂ target at 40 μ A and the 10 μ A data (run4778-4779, PS4=7) with TS4 = 15 mV trigger (the Y-axis of data is normalized to ΔT and the beam current 40 μ A, and the X-axis of data is scaled to the deposit energy based on the MIP peaks. $(0.949 * Shower_l + Shower_r + Shower_t) * 0.11$). The total number of the 10 μ A random trigger runs presented here is 17. So the total ΔT of the random trigger events is $17 * 100k * 400ns = 0.68s$, and each random triggered event in the plot normalized to the total ΔT to the rate to compare with the simulation.

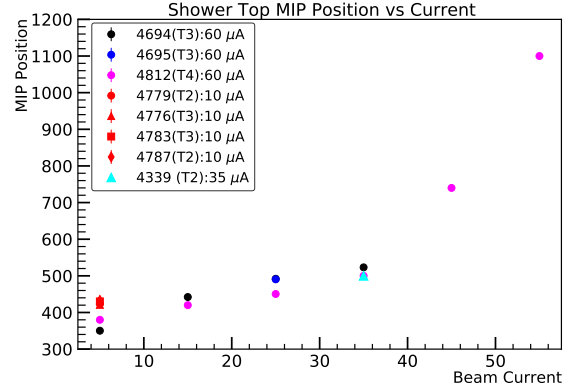


FIG. 11. Shower MIP peak integral in FADC unit vs. beam current for the Top module, showing a significant increase beyond 10-15 μ A.

B. Performance of shower passive base at high rate

During the beam test, it was found the MIP peak position (integrated area) shifted dramatically with the beam current, see Fig. 11. To investigate if the observed MIP peak integral shift is due to pile up, we broke down the contribution from: signal baseline increase due to high background pileupe, signal height, and signal width. While a slight increase in the baseline level was observed, we found the MIP peak shape (width) to remain quite stable and the MIP peak shift was primarily due to the peak height change. This height change can be attributed to the gain change of the PMTs and the cause can be traced down to the use of a passive HV divider.

In fact, a similar situation happened to the Fall 2023 running of the NPS experiment in Hall C. The NPS group found the calorimeter PMT gain would vary when a passive divider is used. To accommodate for the high rate of the NPS experiment, an active base of $\times 12$ pre-amp was used and their PMTs are operated at a low gain of 10^3 . For SoLID situation, while our calculation shows that PMTs of $(1 - 2) \times 10^5$ gain can identify MIP peak while keeping maximal electron energy within the FADC range, our test results indicate that we should consider a similar approach as the NPS calorimeter. That is, using active bases and operate the PMT at the $\approx 10^4$ gain level. Needless to say, one must be careful in the choice of divider component and material and ensure all components are radiation resistant.

C. Timing with FADC

The sampling nature of the FADC allows the extraction of peak time similar to a Time-Digital Converter (TDC). The edge-finding algorithm used in our analysis works as follows (Fig. 12): First, a peak-finding algorithm is used to find the peak height, which is then combined with the pedestal value (V_{ped}) to calculate the mid-point of the amplitude V_{mid} . Next, the FADC samples just before (SN-1) and just after (SN+1) this mid-point are used to look for the time of the mid-point t_{mid} through interpolation. The grid of the interpolation is 1/64 of the sampling time, and thus the precision of the edge-finding is $4/64 = 0.0625$ ns if there were no statistical fluctuations. The value of t_{mid} is taken as the peak starting time, which does not need time-walk corrections.

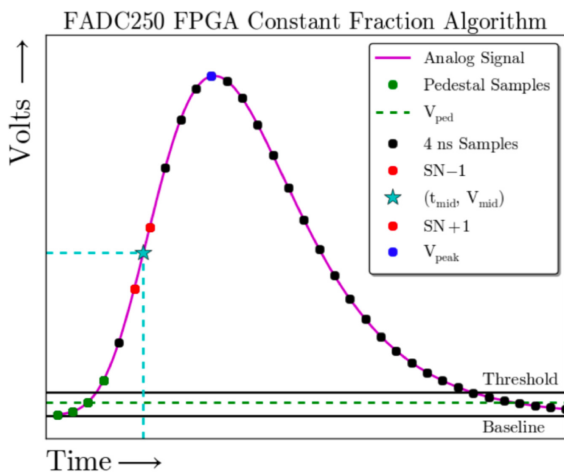


FIG. 12. FADC edge-finding algorithm for extracting the start time of the peak t_{mid} .

We have tested out the timing analysis using scintillator signals from the beam test. However, we found the resolution to be about twice the expected value. To ensure accuracy of the timing measurement during SoLID running, detectors to be used in time-of-flight measurement should be read out by both FADC and dedicated TDC modules.

V. ANALYSIS TO BE COMPLETED

Data analysis is still ongoing and we present below what to be expected once the analysis is complete.

1. GEM tracking analysis: calibration and gain-matching of the GEM chambers have been completed and tracking information is available. The tracking resolution of the beam test

data is not as precise as other experiments (SBS or future SoLID) because of lack of alignment data. However, it is sufficient for our PID analysis, see below.

2. PID performance of LASPD: using beam test data we are able to identify π^0 and photon samples that can be used to extract photon rejection of LASPDs. Our preliminary results are in agreement with the simulated value in which the data sample contains both π^0 and photon, and charged particle background. Work is ongoing to characterize the LASPD PID performance with clean π^0 and photon samples.
3. PID performance of Ecal: using beam test data we are able to identify charged pion samples that can be used to extract the pion rejection of ECal. Our preliminary results are in agreement with the simulated value in which the data sample contains charged pions and background particles. Work is ongoing to characterize the ECal PID performance with clean charged pion samples.
4. While the Cherenkov performance was tested previously and mostly understood, the new beam test data provided additional information to characterize the photo-electron yield of the Cherenkov. This work is ongoing
5. Detailed analysis is ongoing to study the rate dependence of all detectors. We expect to achieve quantitative results on the rate limit of detector performance.
6. Simulation is ongoing that will allow us to compare both rates (signal and background) and radiation dose of the beam test to that of SoLID running.
7. AI/ML-based PID was conducted on simulated data of the beam test. This is to be applied to the actual data and will provide valuable information on how to best implement AI/ML-based PID to SoLID data.

VI. SUMMARY AND OUTLOOK

We report here the SoLID FY22 beam test. A nearly full set of SoLID detector prototypes was placed in Hall C of JLab without magnetic field sweeping and was found to be functioning up to a luminosity of a few $\times 10^{37}$ $\text{cm}^{-2}\text{s}^{-1}$. The observed rates of both signal and background are in agreement with the simulation performed for the specific

beam test setup. Preliminary results show the PID performance of both LASPD (photon rejection) and ECal (charged pion rejection) to be in good agreement with the simulation and that they will satisfy

the requirement of the SoLID physics program. We plan to complete all data analysis with the year 2024. Additional PID analysis using AI/ML method will be carried out if sufficient resources are available.

-
- [1] JEFFERSON LAB SOLID collaboration, J. Arrington et al., *The solenoidal large intensity device (SoLID) for JLab 12 GeV*, *J. Phys. G* **50** (2023) 110501, [2209.13357].
- [2] The SoLID Collaboration, “Solenoidal Large Intensity Device Updated Preliminary Conceptual Design Report.” <https://solid.jlab.org/DocDB/0002/000282/001/solid-precdr-2019Nov.pdf>, 2019.
- [3] C. Peng et al., *Performance of photosensors in a high-rate environment for gas Cherenkov detectors*, *JINST* **17** (2022) P08022, [2011.11769].